Long-term changes in the mesosphere calculated by a two-dimensional model

Aleksandr N. Gruzdev
A. M. Obukhov Institute of Atmospheric Physics, Russian Academy of Sciences, Moscow, Russia

Guy P. Brasseur
Max-Planck-Institut für Meteorologie, Hamburg, Germany

Received 2 December 2003; revised 27 June 2004; accepted 20 July 2004; published 11 February 2005.

[1] We have used the interactive two-dimensional model SOCRATES to investigate the thermal and the chemical response of the mesosphere to the changes in greenhouse gas concentrations observed in the past 50 years (CO_2, CH_4, water vapor, N_2O, CFCs), and to specified changes in gravity wave drag and diffusion in the upper mesosphere. When considering the observed increase in the abundances of greenhouse gases for the past 50 years, a cooling of 3–7 K is calculated in the mesopause region together with a cooling of 4–6 K in the middle mesosphere. Changes in the meridional circulation of the mesosphere damp the pure radiative thermal effect of the greenhouse gases. The largest cooling in the winter upper mesosphere-mesopause region occurs when the observed increase in concentrations of greenhouse gases and the strengthening of the gravity wave drag and diffusion are considered simultaneously. Depending on the adopted strengthening of the gravity wave drag and diffusion, a cooling varying from typically 6–10 K to 10–20 K over the past 50 years is predicted in the extratropical upper mesosphere during wintertime. In summer, however, consistently with observations, the thermal response calculated by the model is insignificant in the vicinity of the mesopause. Although the calculated cooling of the winter mesopause is still less than suggested by some observations, these results lead to the conclusion that the increase in the abundances of greenhouse gases alone may not entirely explain the observed temperature trends in the mesosphere. Long-term changes in the dynamics of the middle atmosphere (and the troposphere), including changes in gravity wave activity may have contributed significantly to the observed long-term changes in thermal structure and chemical composition of the mesosphere.

Citation: Gruzdev, A. N., and G. P. Brasseur (2005), Long-term changes in the mesosphere calculated by a two-dimensional model, *J. Geophys. Res.*, *110*, D03304, doi:10.1029/2003JD004410.

1. Introduction

[2] The mesosphere and, closely related to it, the lower thermosphere are subject to both radiative and dynamical forcings. The radiative budget of this atmospheric region depends crucially on the abundance of radiatively active gases including greenhouse gases (H_2O, CO_2, CH_4, N_2O, and chlorofluorocarbons), which undergo long-term changes due to anthropogenic activity. Atmospheric ozone, which also influences the radiative balance of the middle atmosphere (solar ultraviolet and terrestrial infrared radiation), is strongly affected by changes in dynamical processes. In the mesosphere–lower thermosphere (MLT) region, the dynamical forcing is produced primarily by internal gravity waves [*Houghton*, 1978; *Lindzen*, 1981; *Matsuno*, 1982; *McIntyre*, 2001] emerging into the middle atmosphere mainly from the troposphere [*Holton and Alexander*, 1999; *Gavrilov and Fukao*, 2001; *McIntyre*, 2001]. The significance for the zonal and meridional circulation of dynamical forcing associated with gravity wave (GW) breaking is supported by direct measurements of the GW momentum flux [e.g., *Vincent and Reid*, 1983; *Reid and Vincent*, 1987; *Gavrilov et al.*, 2000] as well as by diagnostic studies [e.g., *Hamilton*, 1983; *Smith and Lyjak*, 1985; *Portnyagin et al.*, 1995].

[3] It is important to emphasize that dynamical forcing in the MLT is related to processes occurring at lower altitudes. The MLT response to changes occurring in the lower atmosphere involves complex interactions between radiative, chemical and dynamical processes. Low air density and small thermal inertia make the MLT very sensitive to changes propagating from beneath, while in the lower atmosphere, the signal can be delayed by decades due to the large inertia of the atmosphere-ocean-cryosphere system. The question of global change signatures in the MLT has been discussed by *Roble* [1995] and *Thomas* [1996a, 1996b].

0148-0227/05/2003JD004410$09.00

[4] The purpose of the present study is to investigate the mechanisms that explain the observed temperature trends in the mesosphere, and specifically the cooling observed in the vicinity of the winter midlatitude mesopause during the past 40 years. Only a limited number of studies have addressed past changes in the MLT region: observations do not provide unambiguous information, and only a few atmospheric models extend up to the lower thermosphere. Before summarizing the major human-driven perturbations that have occurred in the past decades (section 2), and describing the model used to assess the response of the MLT region to these perturbations (section 3), we first review (section 1) the information provided by observations and previous modeling studies. We then present model simulations and discuss model results (sections 4 and 5, respectively). Conclusions are presented in section 6.

1.1. Observed Temperature Changes in the MLT Region

[5] Observations of temperature in the MLT region have been performed using different direct and indirect experimental techniques, and have been used to derive long-term temperature trends over the last decades. The derivation of these trends is not straightforward because the measurements are necessarily limited in time and are affected by natural fluctuations associated for example with atmospheric wave activity or solar variability. The trends at the mesopause level are particularly difficult to derive because of the complex structure of this transition region. Observations in the extratropics show, for example, that the level of the mesopause varies from 87 km during summertime to 100 km during wintertime [*Yu and She*, 1995; *von Zahn et al.*, 1996; *Thulasiraman and Nee*, 2002].

[6] Significant cooling of the mesosphere has been observed, using different measurement techniques [*Kokin and Lysenko*, 1994; *Keckhut et al.*, 1995; *Golitsyn et al.*, 1996; *Taubenheim et al.*, 1997; *Lysenko et al.*, 1999; *Semenov et al.*, 2000; *Bremer and Berger*, 2002]. *Golitsyn et al.* [1996], for example, analyzed a 30-year series (since the mid-1960s) of weekly rocket temperature soundings up to 75 km at a few sites located in the Arctic and the Antarctic, northern midlatitudes, and tropical latitudes. They also studied a 40-year series of hydroxyl airglow measurements at Zvenigorod, Russia (56°N, 37°E). These authors reported a significant cooling in the altitude range of the rocket sounding, with a trend amplitude increasing with height. In the 60–70 km layer, the cooling over 30 years was found to be about 20 K (annual mean temperature), corresponding to an estimated trend of about −0.7 K/year. The annual mean hydroxyl rotational temperatures exhibited for the 40-year observational period a cooling of about 30 K at 87 km (the altitude of the hydroxyl airglow layer), resulting also in a long-term trend about −0.7 K/year in the neighborhood of the mesopause. Using a similar method of measurements, *Bittner et al.* [2002] did not report any trend in an 18-year series of hydroxyl rotational temperature measurements made in Wuppertal, Germany (51°N, 7°E). They noted, however, that their series was too short for deriving a trend because of the large variations in the data. In particular, the temperature at those heights is affected by solar activity, and the Wuppertal data are in agreement with the Zvenigorod data when retrieved with the same method [*Lysenko et al.*, 1999]. The similarity between the trends derived for the stations becomes more obvious after the solar cycle-related variation has been removed from the original signal [*Semenov et al.*, 2002a].

[7] Additional measurements performed over relatively short periods of time have been reported. An 8-year series of hydroxyl emission in northern high latitudes (Sweden) shows a positive temperature trend in winter (no trend in summer) around the mesopause [*Espy and Stegman*, 2002]. On the other hand, a significant negative temperature trend (∼−1 K/year) in the hydroxyl airglow layer has been recently reported by *Reisin and Scheer* [2002] for subtropical southern latitudes over Argentina (32°S, 69°W). Their results suggest temperature trends that are similar to those reported in the northern temperate latitudes. The time series recorded in Sweden and Argentina are, however, of short duration or include significant gaps. Because of the solar cycle influence and the natural variability (especially large in the northern hemisphere), only sufficiently long measurements (including at least two solar cycles) are reliable for detecting a long-term trend.

[8] The long-term temperature trend in the mesopause region (in the hydroxyl airglow layer) was also found in certain cases to be season dependent. In their analysis, *Golitsyn et al.* [2000], for example, report a significant trend of about −0.9 K/year during the winter season, but no significant trend for summer at northern temperate latitudes. This seasonal difference provides a critical test for models, which attempt to reproduce the evolution of temperature over the last decades. At lower altitudes, in the mesosphere, however, the temperature trend is negative for all seasons according to 30-year rocket data [*Semenov et al.*, 2000; *Lysenko and Rusina*, 2002]. Observations of the sodium emissions (∼92 km) and atomic oxygen emissions (∼97 km) in the temperate northern latitudes since the late 1950s suggest no summer temperature trends in this region, but a slight positive trend in winter at 97 km [*Semenov et al.*, 2000]. Inferring temperature trends from observations in the airglow brightness is, however, delicate since trends in airglow intensity and in temperature can be different [*Givishvili et al.*, 1996; *Reisin and Scheer*, 2002]. A nearly zero negative temperature trend is also derived from falling sphere measurements in the northern polar summer mesosphere [*Lübken*, 2000]. This result is consistent with the nearly zero trend reported by *Golitsyn et al.* [2000] at the midlatitude mesopause during summer. A positive temperature trend in the northern temperate latitudes in winter and summer is derived from the measurements of the critical frequency f_oE of midday ionospheric E layer (lower thermosphere at ∼108 km). The variability of the data is significant, however, even after filtering out solar cycle-like oscillations [*Semenov et al.*, 2000].

[9] Fifteen years of Rayleigh lidar measurements in France (44°N) have revealed a negative trend of −0.4 K/year in mesospheric temperatures (up to 80 km) [*Keckhut et al.*, 1995]. *Taubenheim et al.* [1997] analyzed a 30-year series of radiowave reflection heights at 50°N, 10°E and derived a column-mean temperature trend in the mesosphere (up to 82 km) of about −0.6 K/year. These estimates are in agreement with trends obtained from rocket measurements [*Golitsyn et al.*, 1996]. Similar trends are also derived from the 40-year indirect phase-height measurements at

Khlungsborn, Germany [*Bremer and Berger*, 2002]. *Burns et al.* [2002], using 7 years of hydroxyl airglow observations over Davis station in Antarctica, derived a winter temperature trend in the neighborhood of the mesopause of about −0.3 K/year. However, the trend is not statistically significant, probably due to insufficient data. Lidar measurements of the vertical distribution of atmospheric sodium covering a period of 30 years show an insignificant linear negative trend in the centroid height of the sodium layer (∼92 km) in Brazil (23°S, 46°W) for the entire period [*Clemesha et al.*, 2004], and hence no significant temperature trend in the SH tropical mesopause region. This result modifies the conclusions (significant negative trend) reached earlier by *Clemesha et al.* [1997] on the basis of observations made over a shorter period of time. Similarly, no long-term trend has been observed in the sodium layer temperature of the northern temperate latitudes, according to 35-year measurements of sodium emission [*Fishkova et al.*, 2001; *Semenov et al.*, 2002b]. Thirty-five-year measurements of green line atomic oxygen emission measurements (97 km altitude) and measurements of the critical frequency of the E layer have been interpreted to suggest that the temperature trend has been positive in the lower thermosphere [*Semenov et al.*, 2002b].

[10] In summary, no definitive and unambiguous conclusions can be drawn for observational temperature time series in the upper mesosphere and mesopause region regarding long-time trends. Data seem to suggest, however, that the lower and middle mesosphere has been cooling persistently over the past 40 years. In the upper mesosphere, the temperature trend seems to have been relatively small and perhaps insignificant over the last 40 years, except during winter at mid and high latitudes where a cooling as large as 0.7 K/year may have occurred near 85–90 km altitude. It is also likely that, as a result of hydrostatic adjustment produced by the cooling of the stratosphere and mesosphere, the temperature at a given geometric altitude in the lower thermosphere has increased with time over the past decades. Data seem to suggest that the zero trend line is located near 90–95 km altitude. We will therefore make the assumption, based on limited observational evidence, that a substantial cooling took place in the upper mesosphere at extratropical latitudes during the last 4–5 decades, but only in winter. It will also be assumed that the temperature trend during the same period of time has been small in the tropical upper mesosphere and in the extratropical mesopause region during summertime. Continuous observations in this atmospheric region are necessary to provide the data needed to evaluate and confirm these assumptions. In the next sections, we will examine different possible mechanisms that could have led to the cooling of the extratropical upper mesosphere in winter.

1.2. Modeling of Temperature Changes in the MLT Region

[11] One of the possible causes for global change in the MLT region is the increase in the abundance of greenhouse gases released at the Earth's surface. Several model studies of the mesosphere have assessed the response of the middle and upper atmosphere to increasing concentrations of greenhouse gases, and specifically of CO_2. Here we summarize only the main conclusions from these studies, while the reader is referred to the more comprehensive reviews made by *Khosravi et al.* [2002] and *Beig et al.* [2003]. The latter paper contains also a summary of the available observational results on trends.

[12] Most of the models have focused on the thermal response of the middle atmosphere to a doubling of CO_2 and, in some studies, of CH_4 concentrations [*Fels et al.*, 1980; *Brasseur and Hitchman*, 1988; *Roble and Dickinson*, 1989; *Berger and Dameris*, 1993; *Portmann et al.*, 1995; *Thomas*, 1996a, 1996b; *Chakrabarty*, 1997; *Akmaev and Fomichev*, 1998; *Khosravi et al.*, 2002]. A few studies have also considered the response of ozone [*Brasseur and Hitchman*, 1988] and of other constituents [*Roble and Dickinson*, 1989; *Khosravi et al.*, 2002; *Chabrillat and Fonteyn*, 2004]. A few studies considered the response of the middle atmosphere to the observed trends in CO_2 [*Akmaev and Fomichev*, 2000; *Akmaev*, 2002] and, additionally, in ozone [*Volodin*, 2000], CH_4 and water vapor [*Chabrillat and Fonteyn*, 2004]. The study by *Khosravi et al.* [2002] takes also into account the 11-year solar cycle, and concludes that the CO_2-related changes in the middle atmosphere over a period of typically 10 years are smaller than the signal generated by the 11-year solar variability.

[13] Although the simulated thermal responses of the MLT region are different among different studies and sometimes contradictory to each other, the general conclusion from the different modeling studies is that the mesosphere has been cooling in response to the increase in greenhouse gases concentration. The magnitude of the predicted cooling, however, is substantially lower than the values reported by several observational studies, including the investigation of *Golitsyn et al.* [1996]. Only *Volodin* [2000] has derived from his model a thermal response in the mesosphere close to the observed cooling, but this author assumed that the percentage ozone decrease in the mesosphere is equal to the observed percentage ozone decrease in the stratosphere. There is, however, no indication that the ozone trend in the mesosphere has been as large. The models accounting for chemical-dynamical-radiative feedbacks do not provide such a large thermal response [*Brasseur and Hitchman*, 1988; *Portmann et al.*, 1995; *Thomas*, 1996a; *Khosravi et al.*, 2002].

[14] Another disagreement between observational and model results is associated with the seasonal amplitude in the temperature changes at the mesopause. Observations do not reveal a significant cooling in the neighborhood of the summer mesopause in temperate and polar latitudes of the northern hemisphere [*Golitsyn et al.*, 2000; *Lübken*, 2000; *Semenov et al.*, 2000]. Models, however, predict a trend in the mesopause temperature that is significantly larger in summer than in winter [*Berger and Dameris*, 1993; *Portmann et al.*, 1995; *Akmaev and Fomichev*, 2000; *Khosravi et al.*, 2002].

[15] The discrepancies between the observed and calculated temperature changes in the MLT region suggest that, if the trends derived from observations are correct, additional mechanisms must be considered to explain the cooling that took place in the MLT region during the last 4–5 decades. Increase in the atmospheric concentrations of greenhouse gases shifts the thermal balance toward lower temperatures. A similar tendency takes place if the ozone content decreases in response to enhanced concentrations of NO_x,

ClO_x, and HO_x radicals. Increases in NO_x, ClO_x, and HO_x concentrations in the MLT should have resulted from the observed increases in the tropospheric N_2O and CFC abundances and, perhaps from an increase in the stratospheric and mesospheric water vapor content [*Oltmans and Hofmann*, 1995; *Chandra et al.*, 1997; *Siskind and Summers*, 1998; *Oltmans et al.*, 2000; *Rosenlof et al.*, 2001]. *Oltmans et al.* [2000] deduced from balloon measurements made at Boulder, Colorado, a positive trend of 1%/year in the stratospheric water vapor mixing ratio during the 1980–2000 period. *Randel et al.* [2004], however, did not derive a significant trend in water vapor for the 1992–2000 period on the basis of the data provided by the HALOE instrument on board of the Upper Atmosphere Research Satellite (UARS). More systematic observations of stratospheric water vapor are urgently needed to quantify short-term variations as well as long-term trends in the concentration of this compound.

1.3. Changes in MLT Circulation

[16] Changes in the circulation of the MLT region could also have been produced by changes in gravity wave (GW) driving in this region. Although there is no established observational evidence of a long-term change in the GW driving (due to the complexity of this problem as well as too short periods of GW observations), there are good reasons to assume that gravity wave forcing has been modified as a result of human perturbations. Even if the strength of GW sources has not changed significantly, the GW spectrum and amplitudes may have changed in the MLT region in response to changes in wave propagation in the lower atmospheric layers. For example, long-term changes in the zonal wind below the MLT should have affected the filtering of the waves that meet critical layer conditions when they propagate upward [*Fritts*, 1984]. The changes in the MLT GW spectrum may have modified the momentum and energy deposition there. The available measurements of wind variances in the MLT attributed to the GW intensity show interannual changes in the GW activity within the nearly 15 years of observations [*Gavrilov et al.*, 2002].

[17] Changes in GW momentum and energy deposition in the MLT, if it occurs, would produce changes in the zonal wind and in the meridional circulation. Associated changes in mean vertical velocities should influence the thermal balance either directly by adiabatic effect or indirectly by changes in the vertical transport of radiatively active species.

[18] At present, there is some experimental evidence of the long-term changes in the MLT circulation in different regions [*Portnyagin et al.*, 1993; *Bremer et al.*, 1997; *Merzlyakov and Portnyagin*, 1999; *Middleton et al.*, 2002]. *Bremer et al.* [1997], for example, analyzed ionospheric drift data and wind measurements by meteor radar (30 years of data) in northern Germany and reported a statistically significant negative trend in the prevailing (daily mean) zonal wind in the lower thermosphere in summer and winter, while spring and autumn trends are small and not significant. Furthermore, *Merzlyakov and Portnyagin* [1999] analyzed 30 years of radar measurements of meteor trails made in Obninsk, Russia (55°N, 37°E), and found statistically significant negative trends in the annual mean prevailing zonal winds and positive trends in the annual mean prevailing meridional winds of the lower thermosphere over Obninsk and over northern Germany. While the magnitudes of zonal wind trends are similar in the two regions, the meridional wind trend is significantly larger over Germany than over Obninsk. The trend in the zonal wind is largest (in amplitude) in winter, while the trend in the meridional wind is largest in summer [see also *Bremer et al.*, 1997]. (At Obninsk the winter trend of the meridional wind is about zero and statistically insignificant.)

[19] It should be noted that 11-year meteor radar measurements at a midlatitude station in the western hemisphere, Saskatoon, Canada (52°N, 107°E), did not show any trend in the annual mean zonal prevailing wind [*Namboothiri et al.*, 1994]. The trend determined for this period of measurements (1980–1990) over the two regions in Germany and Russia is also near zero and statistically insignificant [*Merzlyakov and Portnyagin*, 1999]. Meteor radar measurements in the UK (52°N) for the 1988–2000 period reveal, however, significant positive trends in both the zonal and meridional winds [*Middleton et al.*, 2002]. The sign of the trend in the meridional wind is the same, although the magnitude of the trend is significantly larger in comparison with the two other European regions. The positive trend in the zonal wind is characteristic of the short measurement period: the prevailing zonal wind over Germany and Obninsk has a tendency to increase as well during at least 8 years within this period [*Merzlyakov and Portnyagin*, 1999]. Both the zonal and meridional wind components in the MLT depend on solar activity [*Bremer et al.*, 1997; *Merzlyakov and Portnyagin*, 1999; *Middleton et al.*, 2002], making several decades of data desirable for quantifying long-term trends.

[20] Finally, one should stress that the circulation and temperature of the upper mesosphere are sensitive to planetary wave activity. The observed tendency for a more zonally symmetric vortex in the lower stratosphere in recent years suggests that planetary wave activity may have changed in recent decades (J. D. Mahlman, personal communication, 2003). This effect is not specifically addressed in the present study.

2. Standing of the Problem

[21] The experimental studies reviewed in the previous section point toward the existence of long-term changes in thermal structure as well as in the circulation in the MLT region, especially during wintertime. Several mechanisms, of radiative and dynamical nature should be considered when providing a theoretical explanation for the observed changes. Among them are the increases in the lower troposphere concentrations of carbon dioxide and methane. Although changes in CO_2 are of key importance for the radiative balance, this gas has no direct chemical effect on the atmosphere. This is not the case for methane, since in addition to its radiative effect, this gas also affects the concentration of ozone, another important radiatively active gas. In addition, the possibility for an additional increase in the water vapor abundance beyond the change resulting from the observed methane increase should be considered. Changes in water vapor abundance affect the radiative balance directly and indirectly by influencing ozone chemistry. Another gas, which influences the photochemical

balance of atmospheric ozone (via NO_x) and whose lower tropospheric concentration has been increasing, is nitrous oxide (N_2O). Finally, changes in the concentrations of CFCs, which affect middle atmosphere ozone, must also be taken into account. Increase in the concentrations of these compounds, which are transported upward to the middle atmosphere, affects the radiative balance and the ozone concentration of the stratosphere and mesosphere with impacts on the circulation in these layers, which affects again the vertical transport of the radiatively active species. Another important feature of the long-term atmospheric changes is the increase in the surface and lower troposphere temperatures. These climate-related effects are taken into account as lower boundary conditions in the model. Changes specified in the model simulations are prescribed according to observations, so that results provided by the model can be compared with observations.

[22] The MLT circulation is also affected by changes in the dynamics of remote atmospheric layers including processes associated with gravity waves. Changes in the altitude and frequency of GW breaking in the upper mesosphere should cause changes in vertical transport of greenhouse gases to this region and in diffusive vertical transport of heat from this region. As a result, changes in GW forcing and propagation can produce a cooling effect in the upper mesosphere. Such potential effect will be addressed by a simple sensitivity calculation: by multiplying uniformly the calculated GW drag and the related diffusion coefficient by the same constant factor (see sections 4 and 5.4 for motivation).

3. Description of the Model

[23] The simulations were performed with the two-dimensional model named SOCRATES (Simulation of Chemistry, Radiation, and Transport of Environmentally Important Species), which is an improved version of the model originally described by *Brasseur et al.* [1990]. The model was developed at the National Center for Atmospheric Research (NCAR) in Boulder, Colorado, and the detailed description is available at http://acd.ucar.edu/models/ [see also *Huang et al.*, 1998].

[24] The model extends from 85°S to 85°N with a latitudinal resolution of 5°, and from the Earth's surface to the lower thermosphere (120 km in log-pressure altitude) with a vertical resolution of 1 km. The vertical coordinate is expressed in log-pressure altitude with an atmospheric height scale of 7 km. The lower boundary condition is specified at 2 km for the meridional circulation and at the Earth's surface for the concentrations or fluxes of chemical species. The model takes into account feedbacks between radiation, chemistry, and dynamics. The time steps are 5 days for diabatic heating calculations, and 1 day for dynamical processes (including heat transport). The time step for chemical calculations depends on the duration of day and night at specified latitude and season, and of time of day (being subdivided into shorter intervals at sunrise and sunset). Totally, 14 intradiurnal time steps are used to account for diurnal variations of species concentrations.

[25] The net diabatic heating accounts for solar heating by ozone (UV and visible) and by molecular oxygen, IR cooling by radiatively active gases (CO_2, H_2O, O_3) and chemical heating in the MLT by exothermic reactions involving odd oxygen and odd hydrogen species [*Brasseur and Offermann*, 1986]. Reduction of UV heating due to airglow processes and of chemical heating due to chemiluminescence is also accounted for. Above 60 km, local thermodynamic equilibrium (LTE) does not hold for radiative emissions by CO_2, and the non-LTE parameterization of *Fomichev et al.* [1998] for IR cooling by CO_2 and O_3 is used, while the parameterization of *Fomichev et al.* [1986] is adopted for IR cooling by water vapor.

[26] The model chemistry includes 52 species and 137 gas-phase, 5 heterogeneous (PSC and aerosols), and 46 photodissociation reactions. It uses the chemical reaction parameters as provided by JPL (2000, available at http://jpldataeval.jpl.nasa.gov).

[27] Temperature and wind velocity components are calculated by solving the heat transport equation, streamfunction equation, and thermal wind equation in the framework of the transformed Eulerian mean circulation using log-pressure altitude as a vertical coordinate [see *Garcia and Solomon*, 1983; *Brasseur et al.*, 1990]. In the tropical belt where the thermal wind equation does not hold, the zonal wind is obtained by interpolation in the latitude direction. The dynamical forcing is provided by parameterized dissipation of planetary waves of wave numbers 1 and 2 [*Garcia*, 1991] and by parameterized GW breaking [*Lindzen*, 1981]. Diffusive mixing coefficients in the vertical and meridional directions are generated in relation with the dissipation of gravity and planetary waves, respectively. The forcing of the middle atmosphere planetary waves is specified at 100 hPa through climatological values of the geopotential [*Randel*, 1987]. In the troposphere, the seasonally dependent Eliassen-Palm flux divergence is specified according to the climatology established by *Randel* [1992]. A more comprehensive summary of the model features is provided by *Khosravi et al.* [2002].

[28] Some modifications in the model have been implemented at the Max Planck Institute for Meteorology (MPI) in Hamburg, Germany. They include a more accurate parameterization of the forcing of the meridional circulation by diffusive transport of heat, a more accurate numerical treatment of molecular thermal conductivity, a new numerical solution of the heat transport equation, and the introduction of an exponential gravity wave decay above the turbopause level. This last modification improves the ability of the model to account for gravity wave effects in the MLT region, while satisfying the upper boundary conditions at 120 km. Finally, the MPI version of the model does not include any relaxation of the mesospheric temperature to a prescribed vertical profile, as was used in the earlier versions of the model.

[29] In summary, the model accounts for most of the physical and chemical processes that are significant in the mesosphere. These processes are treated interactively. One shortcoming in our analysis is the lack of treatment of the diurnal tides in the mesosphere. Such treatment requires the use of a three-dimensional model.

4. Description of Model Simulations

[30] Several scenarios were considered in this study. All of them involved a model integration of 10 years, which is

sufficiently long to analyze the effects of greenhouse gas perturbations on the MLT region. The baseline case, corresponding to "present day" conditions, was simulated to provide a reference, to which perturbation scenarios should be compared. The present day lower boundary conditions for greenhouse gas concentrations were chosen to be representative of current observed values.

[31] In cases with perturbed concentrations of greenhouse gases (CO_2, CH_4, N_2O, CFCs), the lower boundary condition and the initial conditions at all points in the spatial domain of the model were changed by a specified factor (see below). Perturbations in greenhouse gas surface concentrations and in surface temperatures correspond to conditions representative of the state of the atmosphere 50 years ago, and were prescribed in accordance with observations. This 50-year time interval corresponds approximately to the duration of the longest observation series used for analysis of trends in the MLT.

[32] Two cases with CO_2 perturbations were first simulated, one with doubled CO_2 concentrations and one with decreased surface concentrations of CO_2. The doubled CO_2 case has been considered for comparison with other modeling studies. In the other case the lower boundary CO_2 mixing ratios were reduced by 16.2% relative to the present values, to represent the CO_2 levels observed 50 years ago (see, e.g., *Ledley et al.* [1999] and http://www.sses.ch/de/treibhaus/).

[33] In scenarios describing past methane changes, the surface mixing ratios of CH_4 were reduced by 26%, to represent the observed values in the early 1950s [*World Meteorological Organization* (*WMO*), 1999; *Ledley et al.*, 1999]. In the case with perturbed N_2O the surface N_2O mixing ratios were diminished by 15% [*WMO*, 1999; *Ledley et al.*, 1999]. In the case designed to assess the perturbations resulting from the injection of CFCs, the concentrations of all CFCs and halons, except CH_3Cl and CH_3Br, were prescribed to be zero for conditions representative of the situation 50 years ago [*Ledley et al.*, 1999]. Surface concentrations of CH_3Cl and CH_3Br were assumed to remain unchanged over the last 50 years, as these gases are primarily of natural origin [see *Brasseur et al.*, 1999].

[34] Additional cases were considered. In an attempt to simulate the effects of a potential past increase in the concentration of stratospheric water vapor, the initial relative humidity specified at the tropopause level in the simulation representing the state of the atmosphere 50 years ago was assumed to be 20% lower than current values. Since the past trends in water vapor are not well documented, this prescribed change is somewhat arbitrary, and is only used as a sensitivity test. This test allows for a change in water vapor mixing ratios that are larger than if only the CH_4 mixing ratio had been modified.

[35] To account for the past changes in the temperatures at the surface and in the lower troposphere, the latitude dependent monthly mean trends in surface temperatures for the 50 previous years were applied to the model, based on the data provided by P. D. Jones (see http://www.cru.uea.ac.uk/cru/data/temperature/). Temperature changes at 1 and 2 km (the lower boundary for temperature and circulation in the model) were obtained by interpolation between the surface temperature changes and the prescribed zero temperature changes at the tropopause.

[36] To study the potential effect of changes in GW forcing over the last 50 years, model cases with decreased and increased GW drag and diffusion were considered. In these scenarios, the GW drag and diffusion calculated with the parameterization of *Lindzen* [1981] and *Holton* [1982] were modified in different ways. Since dynamical feedbacks are taking place in the model, the real response of the GW drag and diffusion to this change can be different than the factor initially applied (if one compares the GW drag and diffusion for a specified model calendar day with those for the same date in the unperturbed scenario). Four cases, where GW drag and diffusion were multiplied by factors of 0.7, 1.3, 1.5, and 2, respectively, were considered for sensitivity tests.

5. Results and Discussion

[37] Before describing and discussing the model results, a remark on the choice of the vertical coordinate should be made. The SOCRATES model uses log-pressure altitude as the vertical coordinate. However, the MLT temperature response to forced perturbations appears differently when represented in geometrical or in log-pressure altitude coordinates. The use of log-pressure altitude can mask real changes in temperature and species concentrations at fixed altitudes, especially in regions with significant vertical gradients of temperature and of species mixing ratios. For example, due to the subsidence of air in the MLT as a result of diabatic cooling produced by CO_2 enhancement, the thermal effect of the lower thermosphere at fixed geometric altitude can be a warming, not a cooling, since in this region the temperature increases rapidly with height. An appropriate comparison of the model estimates with observational results requires that the same coordinate system be used for both types of data. Since most of the observed temperatures are reported in altitude coordinates, all the results of model calculations have been converted to geometrical altitudes.

5.1. Unperturbed State (Present Conditions)

[38] The distributions of several atmospheric quantities calculated for January under unperturbed conditions are shown in Figures 1a–1k as a function of latitude and geometrical altitude. These model results are used as reference distributions and correspond to present-day conditions. The temperature distribution is shown in Figure 1a. The model captures many important features of the observed temperature distribution [*Fleming et al.*, 1990]. For example, it reproduces the stratopause at ~50 km and the mesopause at ~92 km. The summer mesopause is colder than the winter mesopause, in accordance with observations. The model mesopause in summer is by about 10 K colder in the northern hemisphere (NH, not shown) than in the southern hemisphere (SH). However, the calculated temperature of the polar mesopause in summer is by 10–20 K higher than observed. With the adopted parameterization of the GW forcing, the seasonal change in the mesopause height is also less pronounced than suggested by the observation.

[39] Calculated distributions of mixing ratios of ozone, water vapor, and methane for January are shown in Figures 1b, 1c, and 1d, respectively. Ozone profiles are characterized by two altitude maxima, one in the middle

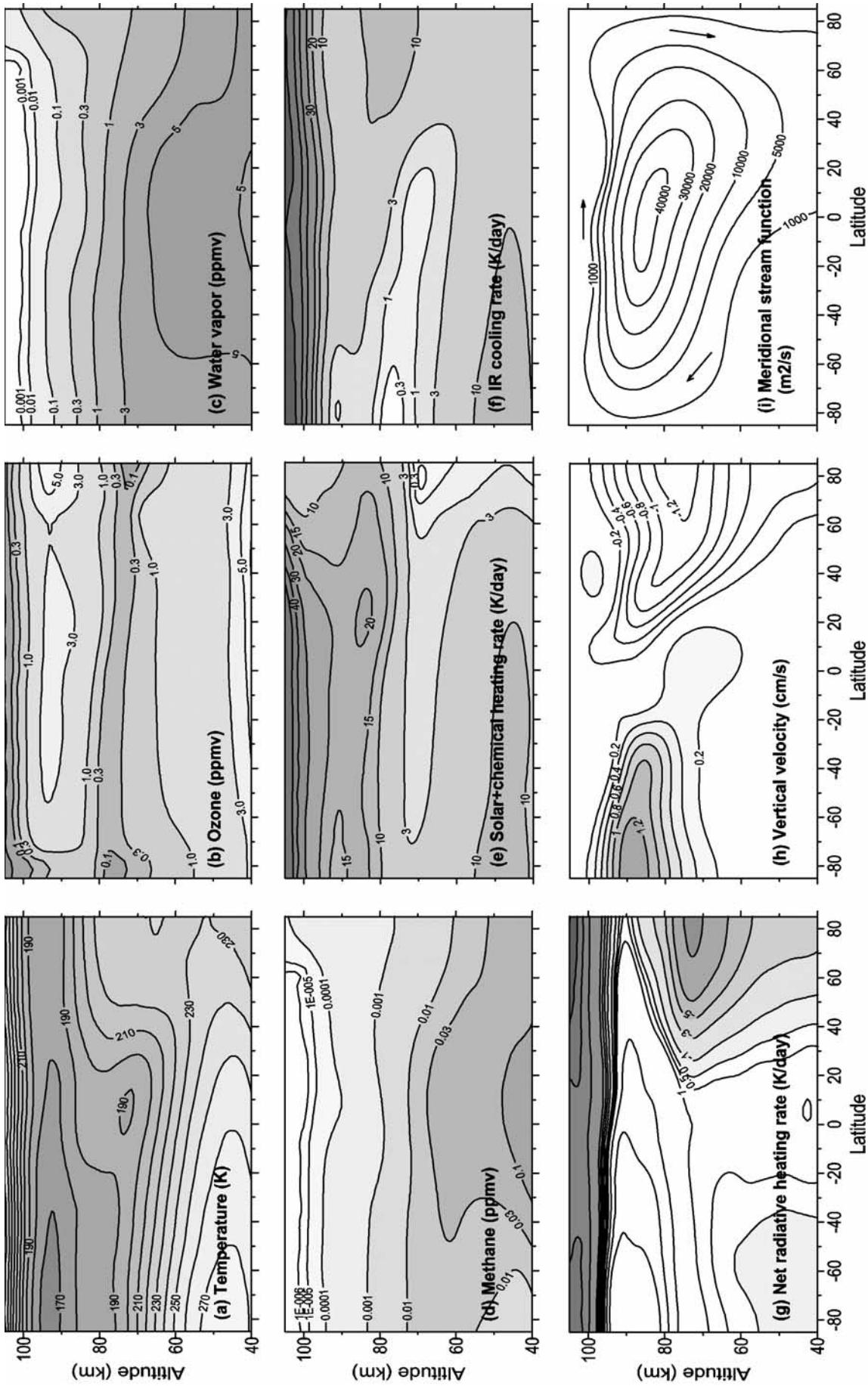

Figure 1. Latitude-altitude distributions of (a) temperature (K), diurnally averaged volume mixing ratios (ppmv) of (b) ozone, (c) water vapor, and (d) methane, diurnally averaged rates (K/day) of (e) diabatic heating (solar + chemical) and (f) IR cooling, (g) diurnally averaged net radiative heating rate, (h) vertical velocity (cm/s), (i) meridional stream function (m^2/s), (j) the vertical diffusive heat flux divergence (K/day), and (k) the total heat flux divergence (K/day) for January.

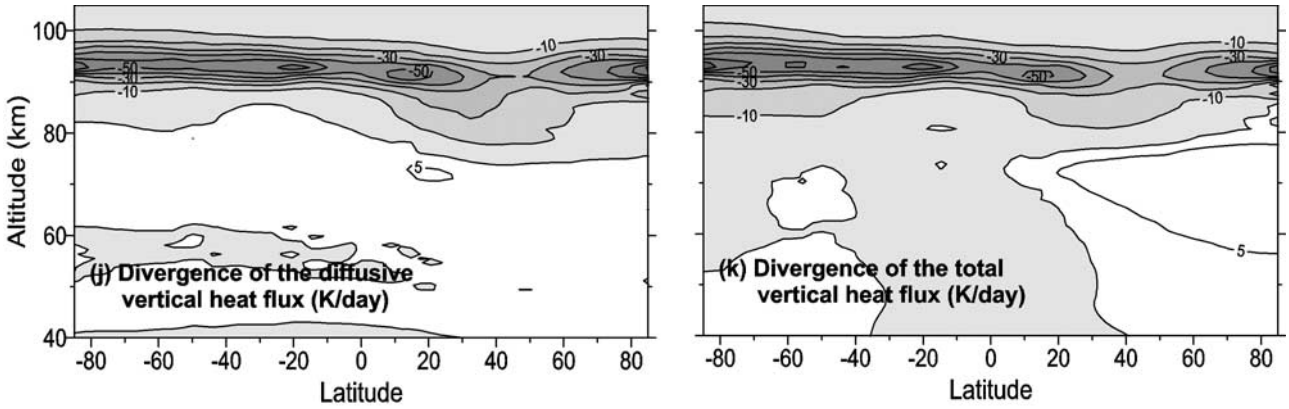

Figure 1. (continued)

stratosphere and another near the mesopause level. The ozone minimun at 70–80 km corresponds to the altitude where the hydroxyl volume mixing ratios reach maximum values. Characteristic for the water vapor distribution shown in Figure 1c is a local maximum in the water vapor mixing ratios in the 40–60 km layer. The height of the maximum decreases with latitude. These features are also present in the observations from UARS (the data are available at http://code916.gsfc.nasa.gov/public/analysis/UARS/urap/home.html). The methane distribution (Figure 1d) is also in reasonably good agreement with observations (UARS) and is characterized by a maximum in the tropics. However, the model does not reproduce the double-peak structure sometimes observed in the tropical or subtropical regions.

[40] Main quantities important for the balance of heat are displayed in Figures 1e–1k. Figure 1e shows the diurnally averaged diabatic heating rate for January, due to shortwave solar heating and to chemical heating. Although the solar heating dominates, the chemical heating provides a significant contribution in the upper mesosphere and in the lower thermosphere. The altitude of the maximum solar heating rate around 50 km results from ozone absorption.

[41] The diurnally averaged IR cooling rate for January is shown in Figure 1f and is a strong function of temperature. The net radiative heating rate in the middle atmosphere (Figure 1g) is determined by a difference between the quantities shown in Figures 1e and 1f. It shows that the mesopause layer is radiatively heated, with the warming rate increasing from the winter to summer pole.

[42] Adiabatic heating is mainly due to vertical motion. The distribution of the vertical wind velocity for January is shown in Figure 1h. Areas with upward motion that leads to adiabatic cooling are shaded. In the upper mesosphere and the lower thermosphere, the most intensive vertical motions occur at extratropical latitudes. These vertical motions constitute the ascending and descending branches of the meridional circulation, whose streamfunction is shown in Figure 1i. Positive values of the stream function correspond to a clockwise circulation.

[43] Figures 1g–1i show that both radiative and adiabatic processes lead to warming of the winter mesopause, while in the summer mesosphere the thermal effects of the two processes are opposite to each other. Besides radiative and adiabatic processes, an essential contribution to the heat balance in the upper mesosphere-mesopause region is provided by eddy vertical transport of heat in the region of intense GW breaking. Figure 1j shows the divergence of the vertical diffusive heat flux for January. This component of the heat balance is negative in the upper mesosphere and lower thermosphere; it reaches a maximum absolute value in the mesopause layer. The cooling rate of the mesopause by this dynamical process can exceed the contributions of the radiative components to the heat budget (see Figures 1e and 1f). The divergence of the total vertical heat flux (diffusive and advective components) is presented in Figure 1k, which shows by comparison with Figure 1j that, at the mesopause, vertical motions contribute less to the heat budget than the vertical diffusive transport of heat.

5.2. Doubling of CO_2

[44] Although the CO_2 concentration has increased by only 16% since 1950, we first consider the classic perturbation case in which the present concentration of atmospheric CO_2 is doubled. The calculated temperature response to such a change in the CO_2 concentration is shown in Figure 2 for January and July. Cooling occurs throughout the mesosphere, with two maxima located in the middle (60–70 km) and upper (80–90 km) mesosphere, where the temperature decreases by about 8 K. There is no essential difference in the vertical structure of the thermal response between January and July. The cooling of the layer located below the mesopause is generally more pronounced in January, while the cooling in the middle mesosphere is generally stronger in July.

[45] Unlike in the mesosphere, temperature in the lower thermosphere increases due to hydrostatic adjustment and specifically the subsidence (due to strong mesospheric and stratospheric cooling) of an atmospheric layer with strong positive temperature gradient. Thus a zero temperature trend is derived by the model near 95 km (geometric altitude). When represented on constant pressure levels, however, the temperature in the lower thermosphere decreases at all levels.

[46] The cooling of the mesosphere is not entirely due to radiative processes, and chemical and dynamical processes must be taken into consideration. In summer the net radiative heating rate (solar heating rate + chemical heating rates − infrared cooling rate) can increase in the upper mesosphere, particularly in response to the increase in the ozone concentration associated with the decrease in tem-

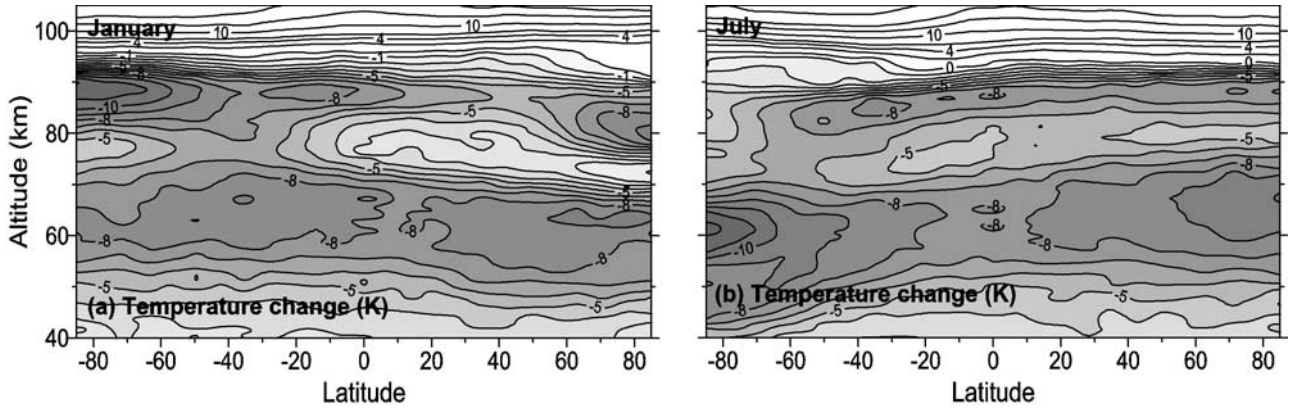

Figure 2. Thermal response (K) of the atmosphere to doubling CO_2 for (a) January and (b) July. Unless otherwise specified, shaded areas, here and in the other figures, correspond to negative changes.

perature (via temperature dependence of chemical reactions) and with the decrease in the atomic hydrogen concentration. This effect leads to a temperature increase in absence of dynamical feedbacks. However, the diabatic heating in the summer upper mesosphere is overcompensated by adiabatic (dynamical) cooling by the meridional circulation, and specifically by stronger upward motion in the summer upper mesosphere. It is worth noting that the change in the radiative balance is also affected by a change in the circulation, which transports radiatively active species. In the winter mesosphere, increased downward motions lead to additional adiabatic warming. The two altitude maxima in the thermal response (Figure 2) result, in part, from the change in the convergence of the vertical heat transport by the meridional circulation.

[47] The calculated response in the winter MLT temperature to a doubling in CO_2 is significantly less than the cooling observed by *Golitsyn et al.* [1996, 2000] over the past 50 years in the extratropics during wintertime (see section 1). Moreover, the large seasonal difference in the mesopause cooling, reported by *Golitsyn et al.* [2000], is not reproduced by the model.

[48] Due to the decrease in the concentration of atomic hydrogen and the subsidence of the MLT region as a result of middle atmosphere cooling (Figure 2), a significant increase in the ozone mixing ratios occurs at constant altitude levels in the upper mesosphere, reaching 20–30% in the SH during summer. Ozone increase of 3–4% occurs also in the upper stratosphere, in the layer with positive vertical ozone gradients (see Figure 1b).

5.3. Fifty-Year Increase in Concentrations of Greenhouse Gases

[49] This section presents calculated impacts of the changes in the concentrations of CO_2, CH_4, N_2O, and stratospheric water vapor over the past 50 years.

5.3.1. Impact of CO_2 Increase

[50] The calculated thermal response of the atmosphere to the increase in the concentration of CO_2 for the past 50 years is shown in Figure 3 for January. The spatial distribution of the response has features that are similar to those shown in Figure 2a, although the amplitudes of the responses in the two figures are different because there is no exact proportionality of the responses. It is worth emphasizing the nonlinearity in the thermal response of the atmosphere to a CO_2 increase. The magnitudes of the increases in surface CO_2 in the two model cases (50-year increase and doubling of present CO_2) differ by a factor of 6, while the temperature changes differ approximately by a factor of 2.5 (compare Figures 2a and 3). The nonlinear character of the response is associated not only with the nonlinearity in the radiative processes but also with nonlinear dynamical-radiative feedbacks. For example, in January the calculated changes in the vertical velocities due to CO_2 increase have different signs in the mesopause layer for the two scenarios. In July the enhancement in the upward motions of the NH is more pronounced for the case with small CO_2 increase than in the CO_2 doubling scenario. The nonlinear thermal response of the atmosphere to a CO_2 increase leads to a saturation of the CO_2 effect for large CO_2 perturbations. A smaller increase in CO_2 cools the atmosphere more effectively than a larger increase. In other words, the thermal sensitivity of the ''present'' middle atmosphere is higher for small changes in CO_2 than for large changes.

5.3.2. Effect of N_2O Increase

[51] The observed increase in the surface concentration of N_2O for the past 50 years leads to an insignificant cooling of the stratosphere and mesosphere. The largest cooling

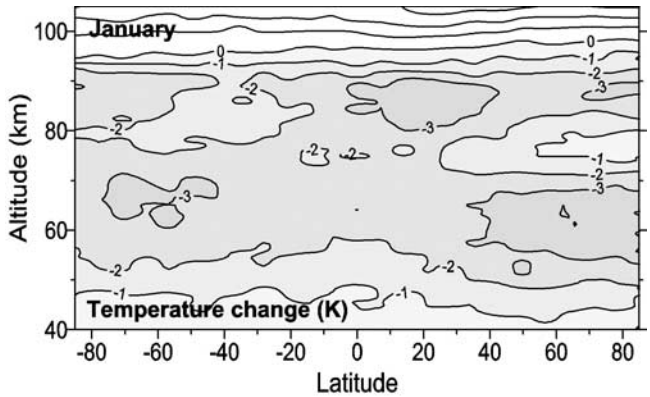

Figure 3. Thermal response (K) of the atmosphere in January to the increase in the suface concentration of CO_2 for the last 50 years.

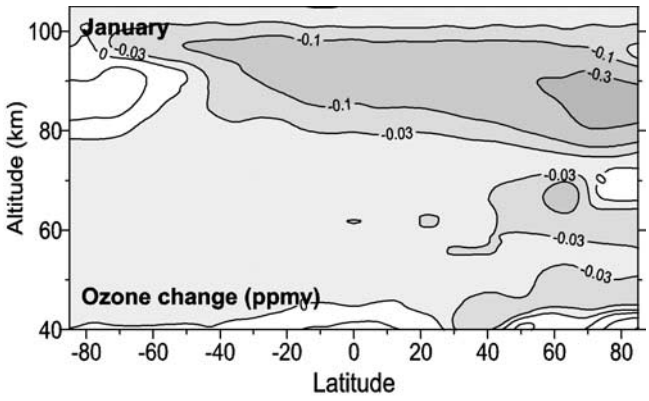

Figure 4. Change in January diurnally mean ozone volume mixing ratios due to the increase in the surface concentration of methane for the last 50 years.

occurs in the middle stratosphere and does not exceed 0.5 K. However, accounting for the N_2O increase can have larger effect in combination with increases in concentrations of other greenhouse gases, due to larger changes in the circulation and, as a result, to N_2O redistribution.

[52] The most important effect of the N_2O increase is a decrease in the ozone concentration, due to the related increase in the NO_x concentration of the middle stratosphere and of the mesosphere. The ozone decrease at the mesopause approaches a few percent.

5.3.3. Effect of CH_4 Increase

[53] Changes in the concentration of methane can affect the concentrations of other species, including water vapor, HO_x, and ozone. The percentage CH_4 increase due to the increase in surface CH_4 concentration over the past 50 years is almost the same throughout the troposphere, but is generally reduced with height in the stratosphere and in the mesosphere. An associated increase in water vapor concentration from the middle stratosphere to the upper mesosphere is typically about 6–7% for the last 50 years. This leads to increases in the stratospheric and mesospheric concentrations of radical species belonging to the hydrogen family. The percentage increase in the averaged concentration of atomic hydrogen in the sunlit MLT region has an altitude maximum (up to 8%) near the mesopause. The increase in the hydroxyl radical concentration is less pronounced at the mesopause and is typically 1–2%. However, the magnitude of this change increases at lower altitudes and reaches 4% in the middle stratosphere. In the layer around 80 km the percentage OH increase reaches a local maximum of 5–10%.

[54] Ozone responds to the methane increase throughout the atmosphere. The diurnally mean ozone concentration increases in the troposphere and generally diminishes in the middle stratosphere and above (Figure 4). The maximum absolute ozone decrease occurs in the mesopause layer. The percentage ozone decrease at these heights is about 4–6%. The ozone change is negligible in the stratosphere, while in the troposphere the ozone concentration increases on the average by about 6%. The ozone decrease in the mesosphere is due to the increase in the concentrations of hydrogen species, and specifically of atomic hydrogen, which reacts with ozone. The ozone increase in the troposphere is associated with the production of peroxy radicals, which, in the presence of NO_x, shifts the photochemical ozone balance toward larger ozone contents [see, e.g., *Brasseur et al.*, 1999].

[55] The CH_4 increase leads to a general cooling (particularly due to the associated increase in the water vapor abundance and the decrease in the ozone concentration) of the upper stratosphere and the mesosphere. Based on the model calculations, this cooling does not exceed 1 K.

5.3.4. Effect of Additional Increase in Lower Stratosphere Water Vapor

[56] As mentioned above, the abundance of stratospheric water vapor may have increased over the past 50 years more than expected from the observed methane trend over the same period. In order to account for a possible and unexplained increase in the water vapor content of the middle atmosphere over the past 50 years, an additional change (by 20%) in relative humidity was specified at the tropopause level (see section 4).

[57] Figure 5 shows the changes in the water vapor mixing ratio calculated in response to simultaneous increases in relative humidity applied at the tropopause and in the methane concentration applied at the surface. The water vapor abundance increases from the stratosphere to the middle mesosphere, but diminishes in the upper mesosphere and in the lower thermosphere, specifically in the region of significant downward motion (compare Figure 5 and Figures 1h and 1i). The typical water vapor increase calculated in the upper stratosphere and the MLT region is in the range of 5–10% (compare Figure 5 and Figure 1c); about a half of it is associated with the methane effect. In the lower stratosphere the water vapor mixing ratio increases by 10–15%. The calculated increase in stratospheric and mesospheric water vapor, however, is lower than the increase which would have taken place if the water vapor trend of ~1%/year reported in Boulder for the 1980–2000 period had been extrapolated for the past 50 years.

[58] The calculated thermal response to this increase in relative humidity applied at the tropopause is a general

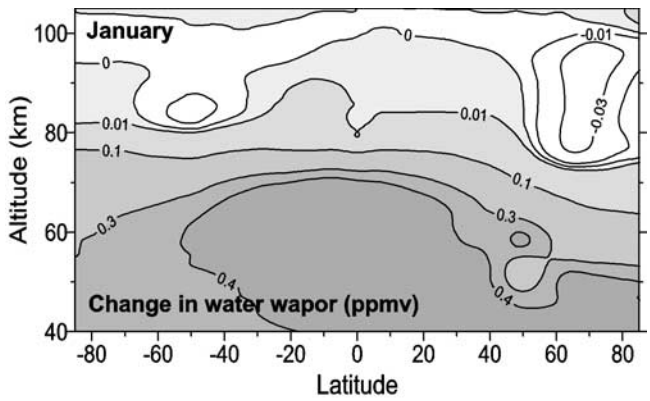

Figure 5. Change in January water vapor mixing ratios due to the 50-year increase in the surface concentration of methane and 20% increase in relative humidity at the tropopause level.

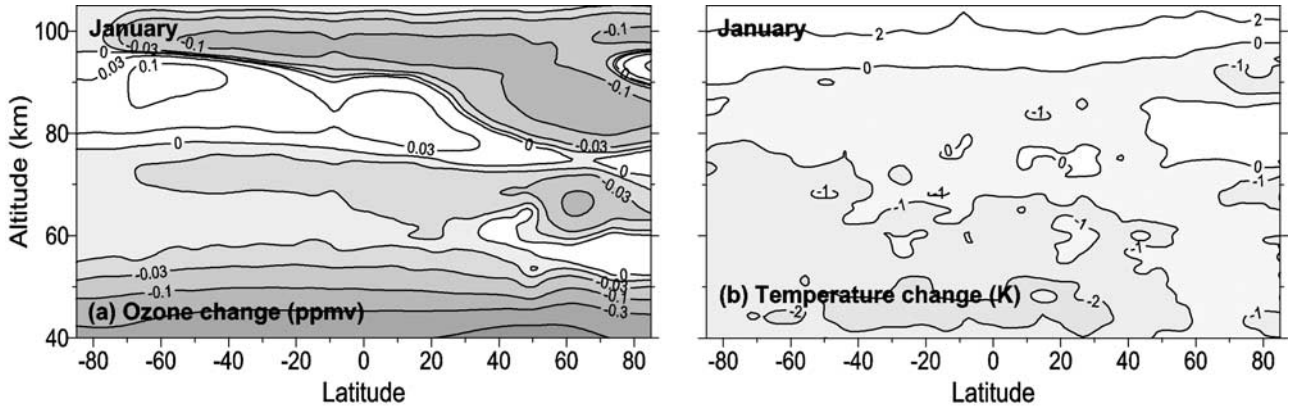

Figure 6. Change (a) in diurnally mean ozone volume mixing ratios and (b) in temperature due to the increase in the surface concentration of CFCs for the last 50 years for January.

cooling of the middle atmosphere, which does not usually exceed 0.5 K, except in the upper mesosphere in the extratropical latitudes of the NH in winter, where it exceeds 1 K.

5.3.5. Effect of Increase in CFCs

[59] The increase in concentrations of anthropogenic halogen compounds from near zero to present values leads to a decrease in the ozone concentration in most parts of the atmosphere (Figure 6a). The largest ozone decrease occurs in the layer around 40 km, where it approaches 20% at midlatitudes of the winter NH. The ozone increase in the layer around 80 km, above the altitude of the ozone minimum (see Figure 1b) is probably associated with the subsidence of the atmosphere (and specifically of atomic oxygen) due to the cooling of the layers below this region (Figure 6b). The decrease in the OH concentration in the upper mesosphere (due in part to the subsidence of the mesospheric hydroxyl layer centered at approximately at 80 km) could also contribute to the ozone increase. The temperature response (cooling) produced by the CFC increase (Figure 6b) is associated primarily with the related ozone decrease. The maximum cooling of about 2 K occurs in the 40–50 km layer in the tropics and in the summer hemisphere.

5.3.6. Combined Effect of Increased Concentrations of Greenhouse Gases

[60] Almost all the perturbations by the individual greenhouse gases have produced a cooling of the mesosphere. A simultaneous increase in the concentrations of greenhouse gases leads to a larger cooling, although the response of the atmosphere is not the arithmetical sum of the individual effects, when treated separately. In this section we consider the response of the atmosphere to the simultaneous increase in the surface concentrations of CO_2, CH_4, N_2O, CFCs over the past 50 years, and in the relative humidity at the tropopause level. The increase in this latter quantity is assumed to be 20% over 50 years.

[61] Figure 7 shows the temperature response to the increase in concentrations of all the listed greenhouse gases, for January and July. In the middle mesosphere, the cooling effect is about 4–6 K. Below the model mesopause (~90 km), it is about 3–4 K, except in the winter northern extratropical latitudes, where this layer is cooled by 5–7 K. Note that the cooling effect of the middle atmosphere over the past 50 years shown in Figure 7 is generally less than the cooling predicted for a CO_2 doubling (compare Figure 2).

[62] The spatial structure of the ozone response resembles that seen in Figure 6a, but the magnitude of the response is slightly larger. An essential feature of the water vapor perturbation in the upper mesosphere is the increase in H_2O mixing ratios in the winter hemisphere (by about 5%) and the decrease of water vapor in the summer hemisphere. The spatial structure of the water vapor perturbation from the upper stratosphere to the middle mesosphere is close to the results obtained for the scenario described in section 5.3.4 (see Figure 5), but the magnitude is somewhat lower. The change in the net radiative heating rate is positive in the upper mesosphere and at the mesopause in all seasons, but is negative in the extratropical latitudes of the NH during winter.

[63] The radiative-dynamical feedbacks cause a response in the circulation of the upper mesosphere-lower thermosphere. In January the dynamical response consists of a strengthening of the meridional circulation (Figure 8). The most important changes in the meridional stream function occur in the winter NH (compare Figure 1i). This results in the strengthening of the downward motion in the northern extratropical latitudes, by up to 0.3–0.4 cm/s in the neighborhood of the mesopause (compare Figure 1h). An associated increase in adiabatic warming in this region (maximum ~1 K) is of the same order of magnitude as the unperturbed net radiative heating rate (cooling, see Figure 1g) and is comparable to the change in the net radiative heating rate resulting from the increase in the concentrations of greenhouse gases (not shown).

[64] An important conclusion from this analysis is that the observed 50-year increase in concentrations of all greenhouse gases under consideration produces a cooling of the upper mesosphere region. An essential aspect of the calculated temperature response for this particular scenario is the larger NH extratropical cooling of the mesopause layer in winter than in summer (compare Figures 7a and 7b). Another conclusion is that the changes in the meridional circulation produce an adiabatic heating that compensates the increased diabatic cooling of the upper mesosphere in winter in the NH. Such a negative feedback maintains the

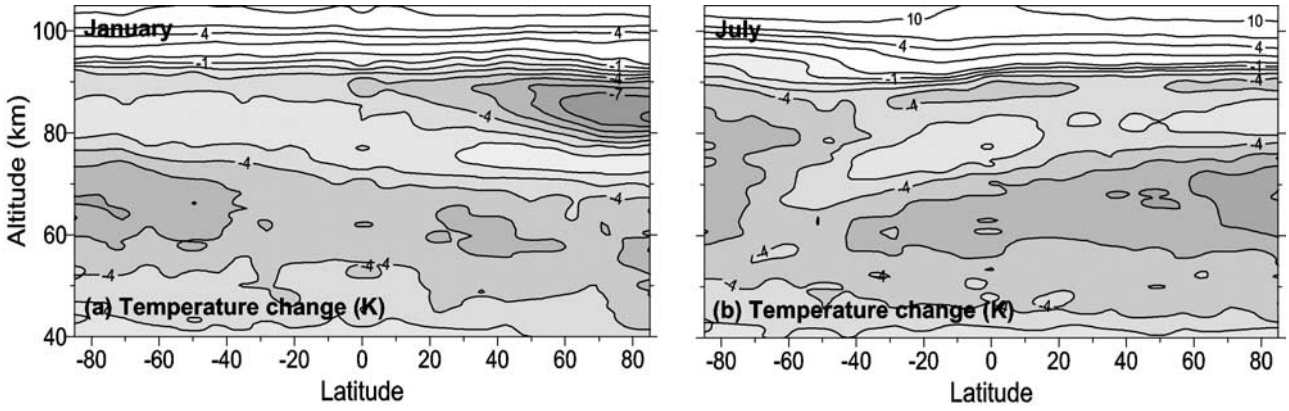

Figure 7. Temperature change (K) due to the increase in concentrations of greenhouse gases for the last 50 years for (a) January and (b) July.

thermal response of the mesosphere to relatively low amplitude.

5.4. Changes in Gravity Wave Forcing

[65] In this section we only consider the potential effects resulting from changes in the GW driving of the MLT region. For reasons mentioned in section 1 and due to the formalism adopted for the GW parameterization (see critical review of different parameterizations of GWs by *Hamilton* [1999]), the changes in GW forcing are implemented in a simple way: by multiplying uniformly the calculated GW drag and the related diffusion coefficient by the same constant factor (see section 4).

[66] Calculations show that a prescribed reduction in the GW drag and associated diffusion results generally in a warming of the upper mesosphere. A prescribed amplification of GW drag and diffusion leads generally to a cooling of this region. Furthermore, an increase in GW-related diffusion provides more effective vertical diffusive transport of greenhouse species to the upper mesosphere-mesopause region and therefore favors a shift of the radiative balance toward lower temperatures. Additional thermal effects can be produced by a change in the vertical diffusive transport of heat in the layers where GWs are breaking (usually in the upper mesosphere-mesopause region). If the GW-related diffusion coefficient increases, more effective downward transport of heat occurs, which results in a cooling of this region.

[67] The response of the calculated meridional circulation to a change in GW drag and diffusion is strongly nonlinear. Figures 9a–9b show the calculated changes in the vertical velocity due to the strengthening of the GW drag and diffusion by factors of 1.3 and 1.5, for January. In the case of the smallest amplification factor (Figure 9a), the downward motion in the mesopause layer becomes stronger in the NH high latitudes, while in the SH the upward motion in the extratropical latitudes becomes weaker (see Figure 1h). The horizontal structure of the changes in the vertical velocity in the upper mesosphere-mesopause layer calculated when the largest factor is adopted (Figure 9b) is almost opposite to that exhibited in Figure 9a for the smallest factor.

[68] Probably, most important for the thermal balance of the upper mesosphere are the changes in diffusive transport of radiatively active species and of heat. The vertical diffusion coefficient associated with gravity wave breaking increases significantly (by up to 20–40%) at mid and high latitudes in the two cases discussed above. As a result, a significant increase in water vapor concentration occurs in the mesopause layer. However, the percentage increase in the water vapor concentration drops rapidly with decreasing altitude. The change in the divergence of the diffusive vertical heat flux in response to the strengthening of the GW drag and diffusivity by a factor 1.3 is shown for January in Figure 10. Increased vertical diffusion in the region of intense GW breaking leads to more effective downward diffusive transport of heat from this region (in the direction opposite to the gradient of potential temperature). It also produces a cooling that can reach 10 K/day at the extratropical mesopause.

[69] The temperature response to the strengthening of the GW drag and diffusion is shown for January in Figures 11a and 11b, respectively, for the two amplification factors, 1.3 and 1.5. The spatial structures of the temperature responses are similar in both cases, except in the neighborhood of the mesopause in the SH summer extratropical latitudes. The middle and upper SH mesosphere (summer) is cooled by about 2 K (see Figure 11a). The cooling of the middle

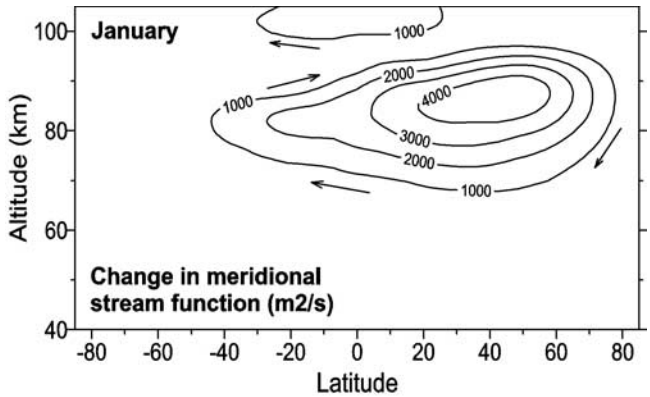

Figure 8. Change in meridional stream function (m^2/s) due to the increase in concentrations of greenhouse gases for the last 50 years for January.

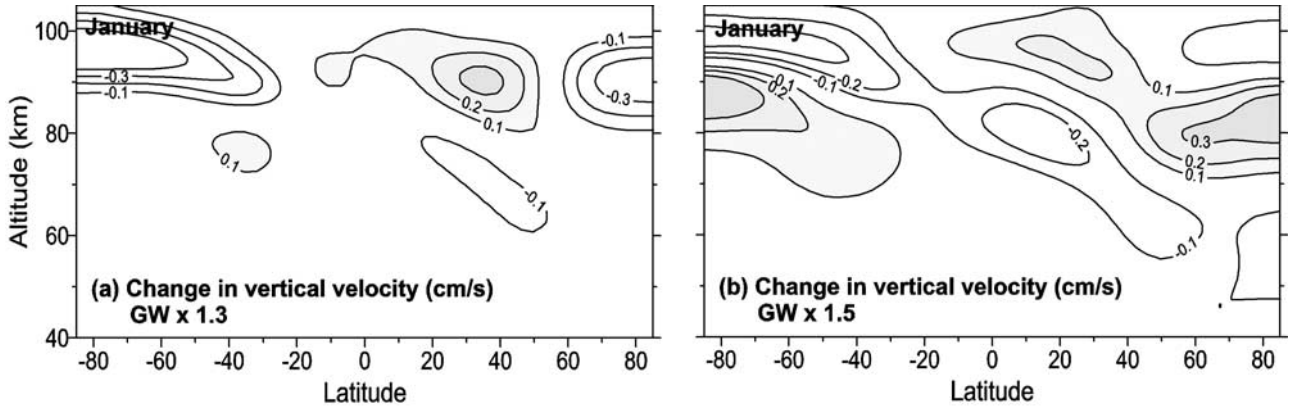

Figure 9. Change in vertical velocity (cm/s) due to the strengthening of the gravity wave drag and diffusion by a factor of (a) 1.3 and (b) 1.5 for January. Areas with positive changes furthering adiabatic cooling are shaded.

summer mesosphere increases with the GW amplification factor, but there is no cooling in the neighborhood of the summer mesopause (Figure 10b).

[70] In the winter hemisphere an increase in GW driving leads to a cooling of the upper mesosphere-mesopause region, and a warming of the stratosphere and of the lower mesosphere. Both effects increase with increasing GW forcing. It is likely that the warming effect in the stratosphere and the lower mesosphere during winter is associated with the strengthening of the downward motion in these regions of the atmosphere (corresponding to negative values in the NH in Figure 9), and with the increase in the poleward meridional winds (not shown). Both effects result in a more intense transport of heat into this region. The warming effect in this stratosphere/lower mesosphere becomes even larger when the GW drag and diffusion are doubled. This warming effect contradicts the observed long-term negative temperature trends observed in the middle atmosphere. It probably results from the way the changes in the GW drag and diffusion are prescribed, which, in the present model case, is not very sensitive to the change in the structure of the atmosphere below the layer of GW breaking. Therefore the analysis of the calculated response of the atmosphere to a prescribed change in GW driving should not be extended far away from the upper mesosphere-lower thermosphere region.

[71] In summary, changes in gravity wave forcing can have a significant cooling effect in the upper mesosphere during winter. The calculated changes can be as large as or even larger than the changes produced by the increase in the concentrations of greenhouse gases. Cooling in the summer mesosphere is small or does not occur.

5.5. Simultaneous Increase in Concentrations of Greenhouse Gases and Strengthening of Gravity Wave Forcing

[72] The temperature response to the simultaneous increase in the concentrations of greenhouse gases for the last 50 years and the strengthening of the GW drag and diffusion by a factor of 1.3 is shown in Figure 12 for January and July. The cooling of the upper mesosphere in the NH extratropical latitudes approaches 5–10 K in winter and is only about 2 K in summer. This calculated seasonal difference in the cooling corresponds qualitatively to the observations of *Golitsyn et al.* [1996, 2000] (see section 1). It should be noted that the same feature is also revealed, when the temperature changes are represented as a function of the log-pressure altitude coordinate.

[73] Figure 13 shows the temperature response in January for the case in which the GW strengthening factor is equal to 1.5. In this case, the winter cooling in the upper mesosphere of the NH extratropical latitudes approaches 7–15 K. The cooling at the summer mesopause is less than 2 K. In the case of a doubled GW drag and diffusion, this region is cooled by 10–21 K (not shown) during winter.

[74] As discussed in section 5.3, the change in the meridional circulation associated with increased GW forcing does not lead usually to a reduction in the adiabatic warming in the NH upper mesosphere. In the cases considered in this section, an intensification of the subsidence branch of the meridional circulation occurs for all GW strengthening factors. As a result, adiabatic warming increases. Therefore the temperature decrease predicted by the model must result from radiative processes and diffusion

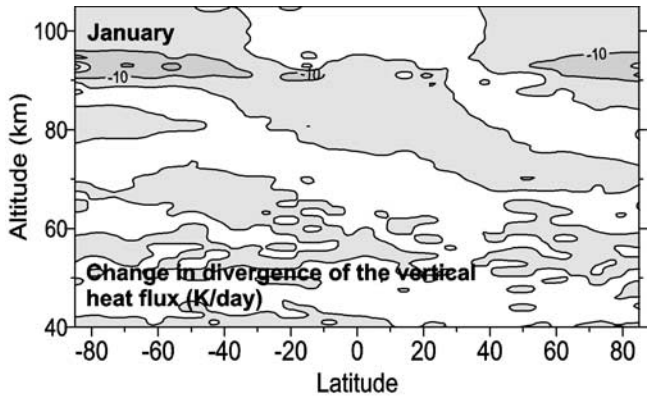

Figure 10. Change in the divergence of the vertical heat flux (K/day) due to the strengthening of gravity wave drag and diffusion by a factor 1.3 for January.

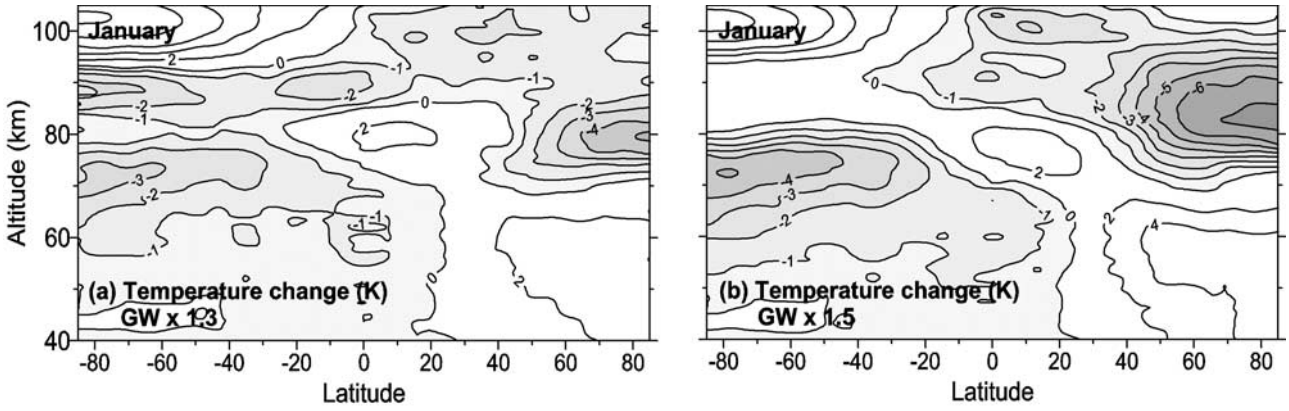

Figure 11. Change in temperature (K) due to the strengthening of the gravity wave drag and diffusion by a factor of (a) 1.3 and (b) 1.5 for January.

transport of heat from the upper mesosphere-mesopause region.

[75] The enhanced diffusive transport associated with GW breaking leads to an increase in the abundances of species whose mixing ratios diminish with height. Concentrations of methane and water vapor undergo significant increase, by tens percent, in the mesopause layer (Figures 14b and 14c). Unlike them, the concentration of CO_2 is not significantly influenced by GW-related diffusion, since the CO_2 mixing ratio is characterized by a small vertical gradient in the middle atmosphere. For completeness, Figure 14a presents percentage increase in CO_2. This increase is almost entirely due to the increase in surface CO_2 concentration, not to the increase in GW-related diffusion.

[76] The increase in the concentrations of greenhouse gases shifts the radiative balance of the upper mesosphere-mesopause layer to lower temperatures. Another effect of the strengthening of GW-related diffusion (which usually occurs in the mesopause layer) is an increase in the divergence of the downward diffusive flux of heat, which also produces a cooling effect (Figure 14d). This cooling mechanism of the mesopause is more effective if the concentration of greenhouse gases increases (see Figure 10).

[77] Results of this section suggest that the changes produced by GW driving can potentially be as important to explain the cooling of the upper mesosphere and the mesopause reported by *Golitsyn et al.* [1996, 2000], as the observed changes in the concentrations of greenhouse gases. The very crude sensitivity test adopted here to assess the impact of changing GW drag and diffusion indicates that changes in GW breaking frequency and intensity could have during winter a cooling effect of the same magnitude as the cooling produced by greenhouse gases in the upper mesosphere-mesopause layer.

[78] Finally, it should be noted that the maximum calculated cooling effect in NH winter is located below the mesopause (Figures 12a and 13). The location of this maximum cooling is quite close to the height of the layer of hydroxyl emission (~87 km), which has provided the main volume of information regarding temperature trends in the neighbourhood of the mesopause (see section 1). It should be also noted that the model does not predict any significant temperature change in the 92–95 km layer, in good agreement with observations [*Semenov et al.*, 2000; *Reisin and Scheer*, 2002].

6. Summary and Conclusions

[79] We have used the two-dimensional model SOCRATES to assess the response of the mesosphere to the observed

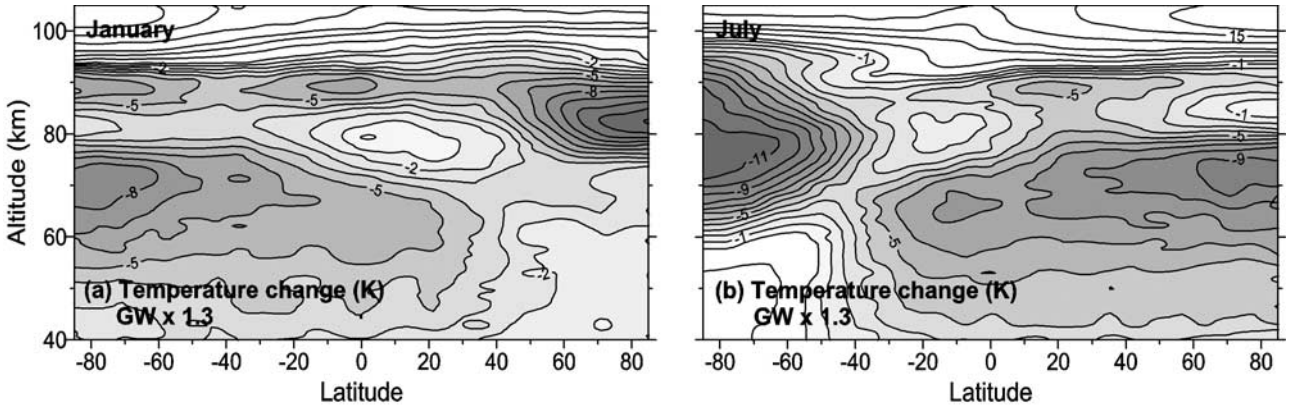

Figure 12. Change in temperature (K) due to the increase in concentrations of greenhouse gases for the last 50 years and the strengthening of the gravity wave drag and diffusion by a factor of 1.3 for (a) January and (b) July.

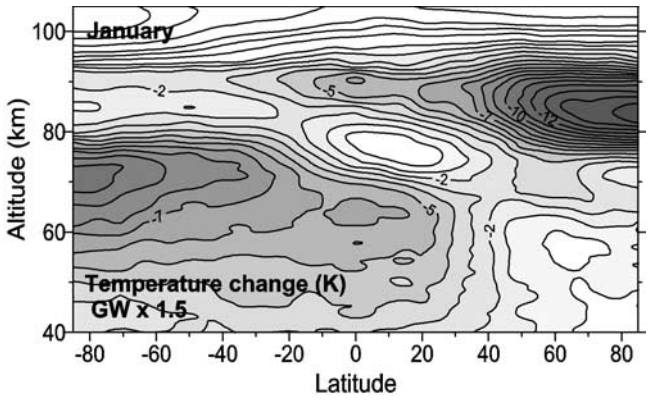

Figure 13. Change in temperature (K) due to the increase in concentrations of greenhouse gases for the last 50 years and the strengthening of the gravity wave drag and diffusion by a factor of 1.5 for January.

increase in tropospheric concentrations of greenhouse gases and to the possible effect of changing GW activity. The model is suited for such investigations since it simulates most of the important radiative, chemical, and dynamical processes that take place in the middle atmosphere. It treats the feedback between these processes interactively. Because the model is two-dimensional, it does not account, however, for the impact of perturbed mesospheric tides, which can have an important effect on the upper mesosphere. Another limitation of our model is associated with the simplified (parameterized) treatment of GW effects. Our results have shown the following.

[80] 1. The doubling of the present surface concentration of CO_2, which is expected to occur over the next several decades, leads to a cooling of the entire mesosphere (in geometrical altitude coordinate). This cooling reaches a maximum between 85 and 90 km altitude, as well as in the 60–70 km layer. The typical cooling in the submesopause region is about 7 K. The largest submesopause cooling (up to 10–11 K) is predicted at high latitudes during winter (January). The middle mesosphere (60–70 km) cools by typically ~8 K while a cooling of 9–11 K is predicted at high latitudes in July. The calculated mesospheric cooling produced by the past 50 year increase in the concentration of CO_2 is smaller than the cooling calculated for a CO_2 doubling.

[81] 2. When taken separately, the observed increase in the concentrations of greenhouse gases other than CO_2 for the past 50 years also leads, in general, to a cooling of the mesosphere, but of less magnitude than in the case of the CO_2 doubling. When considered together, the increases in concentrations of all greenhouse gases (including CO_2) lead to a cooling of the upper mesosphere by typically by 3–4 K, except in the NH extratropical latitudes in winter, where the cooling reaches 5–7 K (80–90 km). The middle mesosphere (60–70 km) has cooled by up to 5 K in all seasons.

[82] 3. When gravity wave drag and diffusion are uniformly enhanced by different factors, a cooling of the NH winter upper mesosphere of several kelvins is predicted by

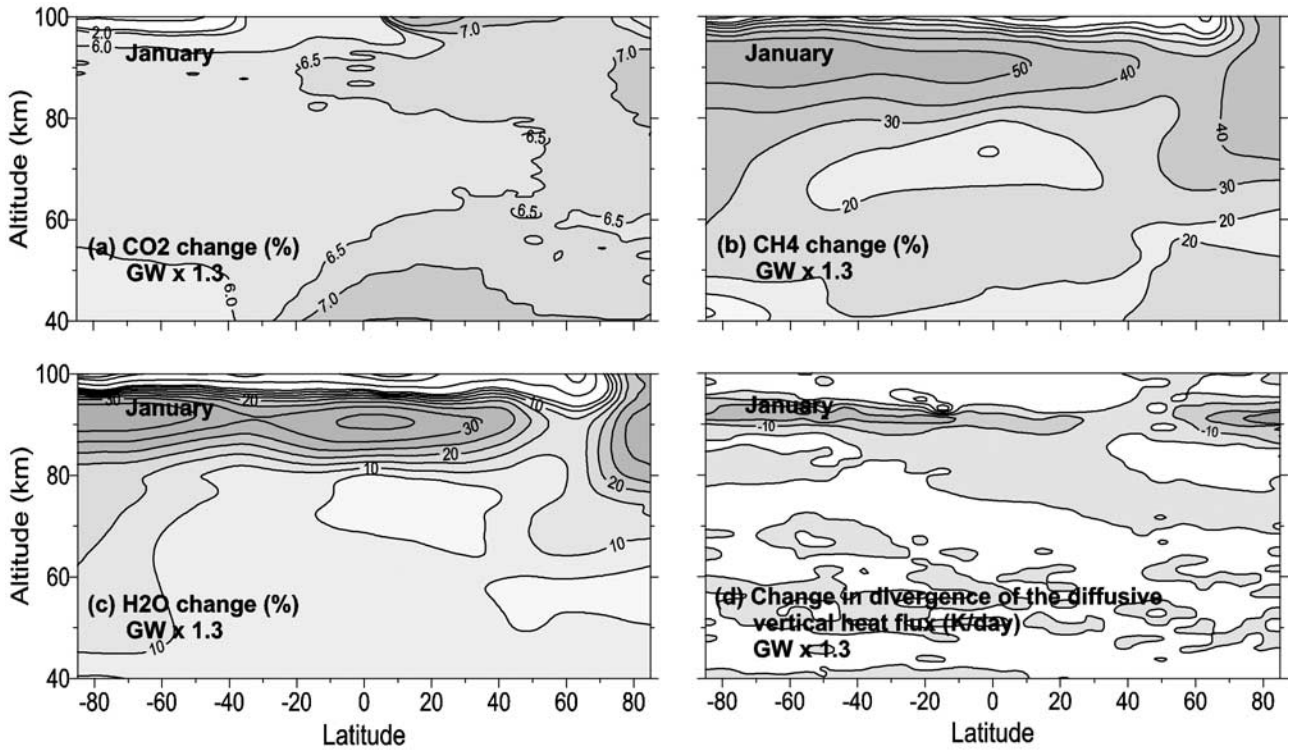

Figure 14. Change (%) in concentrations of (a) CO_2, (b) CH_4, and (c) water vapor, and (d) change in the divergence of the vertical heat flux (K/day) due to the increase in concentrations of greenhouse gases for the last 50 years and the strengthening of the gravity wave drag and diffusion by a factor of 1.3 for January. In Figures 14a–14c, areas with positive changes are shaded.

the model. When the observed increase in concentrations of greenhouse gases and the strengthening of the GW drag and diffusion are accounted for together, the larger cooling occurs in the winter upper mesosphere-mesopause region. In good agreement with observations, the thermal response of the mesopause is small in summer, but becomes significant (cooling ~10 K and more) in the middle mesosphere. In the case of the weakest strengthening of GW drag and diffusion (factor of 1.3), the cooling effect in the extratropical NH near-mesopause layer approaches 6–10 K in winter. Larger amplifications of the GW drag and diffusion result in larger cooling of the winter mesopause. The cooling effect at the mesopause results from the significant increase in the concentrations of methane and water vapor in the upper mesosphere and from the increase in the divergence of the vertical (downward) diffusive flux of heat in this region. Adiabatic warming resulting from the calculated changes in meridional circulation in the MLT, associated both with the increase in concentrations of greenhouse gases and with strengthening of the GW drag and diffusion, tends to compensate the diabatic effect produced by these processes.

[83] 4. The model does not predict any significant temperature change in the 92–95 km layer, and is therefore consistent with the observations of *Semenov et al.* [2000] and of *Reisin and Scheer* [2002]. In the lower thermosphere, the model predicts a warming at constant geometric altitude levels in qualitative agreement with observations at NH midlatitudes [*Semenov et al.*, 2002b].

[84] 5. The winter mesosphere cooling predicted by the model in response to an increase in the CO_2 concentration is significantly less than the cooling reported by *Golitsyn et al.* [1996, 2000]. Moreover, a saturation effect is noticeable: the rate of change in the temperature is reduced when CO_2 is increased beyond a certain value. The same conclusion can be drawn when the observed changes in the abundance of all greenhouse gases over the past 50 years are taken into account in the model. This case did not produce the increase in water vapor concentration in the middle atmosphere reported by *Oltmans et al.* [2000], and thus the diabatic effect resulting from the water vapor increase may be underestimated in our results.

[85] In summary, gravity wave breaking influences effectively the distributions of chemical species and the vertical diffusive transport of heat in the upper mesosphere-lower thermosphere. Strengthening of the GW drag and related diffusion leads to a cooling of the upper mesosphere and of the mesopause. The combined effects of the greenhouse gas concentration increase and of the GW drag and diffusion strengthening leads to model results that are in closer agreement with the observed long-term cooling of the upper mesosphere (and of the middle mesosphere in summer). However, the calculated cooling at the winter mesopause is still lower than observed by *Golitsyn et al.* [1996, 2000] in the NH temperate latitudes. Like other model cases, this scenario underestimates also a possible thermal effect produced by the possible increase in water vapor abundance in the middle atmosphere during the past 50 years.

[86] Further modeling studies are needed to better assess and explain the cause(s) of the changes that have occurred in the thermal structure and chemical composition of the mesosphere. More experimental information about the variability and long-term changes in the characteristics of gravity waves should also be obtained in the lower atmosphere as well as in the MLT.

[87] **Acknowledgments.** We thank Theresa Y. Huang, Rashid Khosravi, and Simon Chabrillat for their contribution to the development of the current version of the SOCRATES model. We also thank Hauke Schmidt and Claudia Timmreck for useful comments on the manuscript and an anonymous reviewer for very constructive comments. Support for this research was provided by the Max Planck Institute for Meteorology and by Germany Federal Ministry for Education and Research (BMBF), project MEDEC/AFO-2000. This study was also supported (partially for A. N. Gruzdev) by the International Scientific and Technology Center under project 2274.

References

Akmaev, R. A. (2002), Modeling the cooling due to CO_2 increase in the mesosphere and lower thermosphere, *Phys. Chem. Earth*, *27*, 521–528.

Akmaev, R. A., and V. I. Fomichev (1998), Cooling of the mesosphere and lower thermosphere due to doubling of CO_2, *Ann. Geophys.*, *16*, 1501–1512.

Akmaev, R. A., and V. I. Fomichev (2000), A model estimate of cooling in the mesosphere and lower thermosphere due to the CO_2 increases over the last 3–4 decades, *Geophys. Res. Lett.*, *27*, 2113–2116.

Beig, G., et al. (2003), Review of mesospheric temperature trends, *Rev. Geophys.*, *41*(4), 1015, doi:10.1029/2002RG000121.

Berger, U., and M. Dameris (1993), Cooling of the upper atmosphere due to CO_2 increases: A model study, *Ann. Geophys.*, *11*, 809–819.

Bittner, M., D. Offermann, H.-H. Graef, M. Donner, and K. Hamilton (2002), An 18-year time series of OH rotational temperatures and middle atmsphere decadal variations, *J. Atmos. Sol. Terr. Phys.*, *64*, 1147–1166.

Brasseur, G. P., and M. H. Hitchman (1988), Stratospheric response to trace gas perturbations: Changes in ozone and temperature distributions, *Science*, *240*, 634–637.

Brasseur, G. P., and D. Offermann (1986), Recombination of atomic oxygen near the mesopause: Interpretation of rocket data, *J. Geophys. Res.*, *91*, 10,818–10,824.

Brasseur, G., M. H. Hitchman, S. Walters, M. Dymek, E. Falise, and M. Pirre (1990), An interactive chemical dynamical two-dimensional model of the middle atmosphere, *J. Geophys. Res.*, *95*, 5639–5655.

Brasseur, G. P., J. J. Orlando, and G. S. Tyndall (Eds) (1999), *Atmospheric Chemistry and Global Change*, 654 pp., Oxford Univ. Press, New York.

Bremer, J., and U. Berger (2002), Mesospheric temperature trends derived from ground-based LF phase-height observations at midlatitudes: Comparison with model simulations, *J. Atmos. Sol. Terr. Phys.*, *64*, 805–816.

Bremer, J., R. Schminder, K. M. Greisiger, P. Hoffmann, D. Kürschner, and W. Singer (1997), Solar cycle dependence and long-term trends in the wind field of the mesosphere/lower thermosphere, *J. Atmos. Sol. Terr. Phys.*, *59*, 497–509.

Burns, G. B., W. J. R. French, P. A. Greet, F. A. Phillips, P. F. B. Williams, K. Finlayson, and G. Klich (2002), Seasonal variations and interannual trends in 7 years of hydroxyl airglow rotational temperatures at Davis station (69°S, 78°E), Antarctica, *J. Atmos. Sol. Terr. Phys.*, *64*, 1167–1174.

Chabrillat, S., and D. Fonteyn (2004), Modeling long-term changes of mesospheric temperature and chemistry, *Adv. Space Res.*, in press.

Chakrabarty, D. K. (1997), Mesopause scenario on doubling of CO_2, *Adv. Space Res.*, *20*, 2117–2125.

Chandra, S., C. H. Jackman, E. L. Fleming, and J. M. Russell III (1997), The seasonal and long-term changes in mesospheric water vapor, *Geophys. Res. Lett.*, *24*, 639–642.

Clemesha, B., P. P. Batista, and D. M. Simonich (1997), Long-term and solar cycle changes in the atmospheric sodium layer, *J. Atmos. Sol. Terr. Phys.*, *59*, 1673–1678.

Clemesha, B., D. Simonich, P. Batista, T. Vondrak, and J. M. C. Plane (2004), Negligible long-term trend in the upper atmosphere at 23°S, *J. Geophys. Res.*, *109*, D05302, doi:10.1029/2003JD004243.

Espy, P. J., and J. Stegman (2002), Trends and variability of mesospheric temperature at high latitudes, *Phys. Chem. Earth*, *27*, 543–553.

Fels, S. B., J. D. Mahlman, M. D. Schwarzkopf, and R. W. Sinclair (1980), Stratospheric sensitivity to perturbations in ozone and carbon dioxide: Radiative and dynamical response, *J. Atmos. Sci.*, *37*, 2265–2297.

Fishkova, L. M., N. M. Martsvaladze, and N. N. Shefov (2001), Long-term variations of the nighttime upper-atmosphere sodium emission, *Geomagn. Aeron.*, *41*, 528–532.

Fleming, E. L., S. Chandra, J. J. Barnett, and M. Corney (1990), Zonal mean temperature, pressure, zonal wind and geopotential height as functions of latitude, *Adv. Space. Res.*, *10*(12), 11–59.

Fomichev, V. I., G. M. Shved, and A. A. Kutepov (1986), Radiative cooling of the 30–110 km atmospheric layer, *J. Atmos. Terr. Phys.*, *48*, 529–544.

Fomichev, V. I., J. P. Blanchet, and D. S. Turner (1998), Matrix parameterization of the 15 μm CO_2 band cooling in the middle and upper atmosphere for variable CO_2 concentration, *J. Geophys. Res.*, *103*, 11,505–11,528.

Fritts, D. C. (1984), Gravity wave saturation in the middle atmosphere: A review of theory and observations, *Rev. Geophys.*, *22*, 275–308.

Garcia, R. (1991), Parameterization of planetary wave breaking in the middle atmosphere, *J. Atmos. Sci.*, *48*, 1405–1419.

Garcia, R., and S. Solomon (1983), A numerical model of the zonally averaged dynamical and chemical structure of the middle atmosphere, *J. Geophys. Res.*, *88*, 1379–1400.

Gavrilov, N. M., and S. Fukao (2001), Hydrodynamic tropospheric wave sources and their role in gravity wave climatology of the upper atmosphere from the MU radar observations, *J. Atmos. Sol. Terr. Phys.*, *63*, 931–943.

Gavrilov, N. M., S. Fukao, and T. Nakamura (2000), Gravity wave intensity and momentum fluxes in the mesosphere over Shigaraki, Japan (35°N, 136°E) during 1986–1997, *Ann. Geophys.*, *18*, 834–843.

Gavrilov, N. M., S. Fukao, T. Nakamura, C. Jacobi, D. Kürschner, A. M. Manson, and C. E. Meek (2002), Comparative study of interannual changes of the mean winds and gravity wave activity in the middle atmosphere over Japan, central Europe, and Canada, *J. Atmos. Sol. Terr. Phys.*, *64*, 1003–1010.

Givishvili, G. V., L. N. Leshchenko, E. V. Lysenko, S. P. Perov, A. I. Semenov, N. P. Sergienko, L. M. Fishkova, and N. N. Shefov (1996), Long-term trends of some characteristics of the Earth's atmosphere. I. Experimental results, *Izv. Atmos. Oceanic Phys.*, *32*, 303–312.

Golitsyn, G. S., A. I. Semenov, N. N. Shefov, L. M. Fishkova, E. V. Lysenko, and S. P. Perov (1996), Long-term temperature trends in the middle and upper atmosphere, *Geophys. Res. Lett.*, *23*, 1741–1744.

Golitsyn, G. S., A. I. Semenov, and N. N. Shefov (2000), Seasonal variations of the long-term temperature trend in the mesopause region, *Geomagn. Aeron.*, *40*, 198–200.

Hamilton, K. (1983), Diagnostic study of the momentum balance of the Northern Hemisphere winter stratosphere, *Mon. Weather Rev.*, *111*, 1434–1441.

Hamilton, K. (1999), The GW parameterization problem for global simulation models, *SPARC Newsl.*, *12*, 7–14.

Holton, J. R. (1982), The role of gravity-wave-induced drag and diffusion in the momentum budget of the mesosphere, *J. Atmos. Sci.*, *39*, 791–799.

Holton, J. R., and M. J. Alexander (1999), Gravity waves in the mesosphere generated by tropospheric convection, *Tellus, Ser. A-B*, *51*, 45–58.

Houghton, J. T. (1978), The stratosphere and mesosphere, *Q. J. R. Meteorol. Soc.*, *104*, 1–29.

Huang, T., et al. (1998), Description of SOCRATES—A chemical dynamical radiative two-dimensional model, *NCAR Tech. Note TN-440+EDD*, 94 pp., Natl. Cent. for Atmos. Res., Boulder, Colo.

Keckhut, P., A. Hauchecorne, and M. L. Chanin (1995), Midlatitude long-term variability of the middle atmosphere: Trends and cyclic and episodic changes, *J. Geophys. Res.*, *100*, 18,887–18,897.

Khosravi, R., G. Brasseur, A. Smith, D. Rusch, S. Walters, S. Chabrillat, and G. Kockarts (2002), Response of the mesosphere to human-induced perturbations and solar variability calculated by a 2-D model, *J. Geophys. Res.*, *107*(D18), 4358, doi:10.1029/2001JD001235.

Kokin, G. A., and E. V. Lysenko (1994), On temperature trends of the atmosphere from rocket and radiosonde data, *J. Atmos. Terr. Phys.*, *56*, 1035–1040.

Ledley, T. S., E. T. Sundquist, S. E. Schwartz, D. K. Hall, J. D. Fellows, and T. L. Killeen (1999), Climate change and greenhouse gases, *Eos Trans. AGU*, *80*, 453.

Lindzen, R. S. (1981), Turbulence and stress owing to gravity wave and tidal breakdown, *J. Geophys. Res.*, *86*, 9707–9714.

Lübken, F.-J. (2000), Nearly zero temperature trend in the polar summer mesosphere, *Geophys. Res. Lett.*, *27*, 3603–3606.

Lysenko, E. V., and V. Y. Rusina (2002), Changes in the stratospheric and mesospheric thermal conditions during the last three decades: 3. Linear trends of monthly mean temperatures, *Izv. Atmos. Oceanic Phys.*, *38*, 296–304.

Lysenko, E. V., S. P. Perov, A. I. Semenov, N. N. Shefov, V. A. Sukhodoev, G. V. Givishvili, and L. N. Leshchenko (1999), Long-term trends of the yearly mean temperature at heights from 25 to 110 km, *Izv. Atmos. Oceanic Phys.*, *35*, 393–400.

Matsuno, T. (1982), Quasi-one-dimensional model of the middle atmosphere circulation interacting with internal gravity waves, *J. Meteorol. Soc. Jpn.*, *60*, 215–226.

McIntyre, M. E. (2001), Global effects of gravity waves in the middle atmosphere: A theoretical perspective, *Adv. Space Res.*, *27*, 1723–1736.

Merzlyakov, E. G., and Y. I. Portnyagin (1999), Long-term changes in the parameters of winds in the midlatitude lower thermosphere (90–100 km), *Izv. Atmos. Oceanic Phys.*, *35*, 482–493.

Middleton, H. R., N. J. Mitchell, and H. G. Muller (2002), Mean winds of the mesosphere and lower thermosphere at 52°N in the period 1988–2000, *Ann. Geophys.*, *20*, 81–91.

Namboothiri, S. P., C. E. Meek, and A. H. Manson (1994), Variations of mean winds and solar tides in the mesosphere and lower thermosphere over timescales ranging from 6 months to 11 years: Saskatoon, 52°N, 107°W, *J. Atmos. Terr. Phys.*, *56*, 1313–1325.

Oltmans, S. J., and D. J. Hofmann (1995), Increase in lower-stratospheric water vapor at a midlatitude Northern Hemisphere site from 1981–1994, *Nature*, *374*, 146–148.

Oltmans, S. J., H. Volmel, D. J. Hofmann, K. Rosenlof, and D. Kley (2000), The increase in stratospheric water vapor from balloon-borne frostpoint hygrometer measurements at Washington, D. C., and Boulder, Colorado, *Geophys. Res. Lett.*, *27*, 3453–3456.

Portmann, R. W., G. E. Thomas, S. Solomon, and R. R. Garcia (1995), The importance of dynamical feedback on doubled CO_2-induced changes in the thermal structure of the mesosphere, *Geophys. Res. Lett.*, *22*, 1733–1736.

Portnyagin, Y. I., J. M. Forbes, G. I. Fraser, R. A. Vincent, S. K. Avery, I. A. Lysenko, and N. A. Makarov (1993), Dynamics of the Antarctic and Arctic mesosphere and lower thermosphere regions – I. The prevailing winds, *J. Atmos. Terr. Phys.*, *55*, 827–841.

Portnyagin, Y. I., J. M. Forbes, T. V. Solovjeva, S. Miyahara, and C. DeLuca (1995), Momentum and heat sources of the mesosphere and lower thermosphere region 70–110 km, *J. Atmos. Terr. Phys.*, *57*, 967–977.

Randel, W. J. (1987), Global atmospheric circulation statistics, 1000-1 mb, *NCAR Tech. Note TN-295*, 245 pp., Natl. Cent. for Atmos. Res., Boulder, Colo.

Randel, W. J. (1992), Global atmospheric circulation statistics, 1000-1 mb, *NCAR Tech. Note TN-366+STR*, 256 pp., Natl. Cent. for Atmos. Res., Boulder, Colo.

Randel, W. J., F. Wu, and S. J. Oltmans (2004), Interannual changes in stratospheric water vapor and correlations with tropical tropopause temperatures, *J. Atmos. Sci.*, in press.

Reid, I. M., and R. A. Vincent (1987), Measurements of mesospheric gravity wave momentum fluxes and mean flow acceleration at Adelaide, Australia, *J. Atmos. Terr. Phys.*, *49*, 443–460.

Reisin, E. R., and J. Scheer (2002), Searching for trends in mesopause region airglow intensities and temperatures at El Leoncito, *Phys. Chem. Earth*, *27*, 563–569.

Roble, R. G. (1995), Major greenhouse cooling (yes, cooling): The upper atmosphere response to increased CO_2, *Rev. Geophys.*, *33*(S1), 539–546.

Roble, R. G., and R. E. Dickinson (1989), How will changes in carbon dioxide and methane modify the mean structure of the mesosphere and thermosphere, *Geophys. Res. Lett.*, *16*, 1441–1444.

Rosenlof, K. H., et al. (2001), Stratospheric water vapor increases over the past half-century, *Geophys. Res. Lett.*, *28*, 1195–1198.

Semenov, A. I., et al. (2000), Seasonal peculiarities of long-term temperature trends of the middle atmosphere, *Dokl. Earth Sci.*, *375*, 1286–1289.

Semenov, A. I., V. A. Sukhodoev, and N. N. Shefov (2002a), A model of vertical temperature distribution in the atmosphere at altitudes of 80–100 km that taking into account the solar activity and the long-term trend, *Geomagn. Aeron.*, *42*, 252–256.

Semenov, A. I., N. N. Shefov, E. V. Lysenko, G. V. Givishvili, and A. V. Tikhonov (2002b), The seasonal peculiarities of behavior of the long-term temperature trends on the middle atmosphere in the midlatitudes, *Phys. Chem. Earth*, *27*, 529–534.

Siskind, D. E., and M. E. Summers (1998), Implications of enhanced mesospheric water vapor observed by HALOE, *Geophys. Res. Lett.*, *25*, 2133–2136.

Smith, A. K., and L. J. Lyjak (1985), Observational estimate of gravity wave drag from the momentum balance in the middle atmosphere, *J. Geophys. Res.*, *90*, 2233–2241.

Taubenheim, J., G. Entzian, and K. Berendorf (1997), Long-term decrease of mesospheric temperature, 1963–1995, inferred from radio wave reflection heights, *Adv. Space Res.*, *20*, 2059–2063.

Thomas, G. E. (1996a), Global change in the mesosphere–lower thermosphere region: Has it already arrived?, *J. Atmos. Sol. Terr. Phys.*, *58*, 1629–1656.

Thomas, G. E. (1996b), Is the polar mesosphere the miner's canary of global change?, *Adv. Space. Res.*, *18*(3), 149–158.

Thulasiraman, S., and J. B. Nee (2002), Further evidence of a two-level mesopause and its variations from UARS high-resolution Doppler imager temperature data, *J. Geophys. Res.*, *107*(D18), 4355, doi:10.1029/2000JD000118.

Vincent, R. A., and I. M. Reid (1983), Doppler measurements of mesospheric gravity wave momentum fluxes, *J. Atmos. Sci.*, *40*, 1321–1333.

Volodin, E. M. (2000), Sensitivity of the stratosphere and mesosphere to observed changes in ozone and carbon dioxide concentrations as simulated by the Institute of Numerical Mathematics atmospheric general circulation model, *Izv. Atmos. Oceanic Phys.*, *36*, 566–573.

von Zahn, U., J. Höffner, V. Eska, and M. Alpers (1996), The mesopause altitude: Only two distinctive levels worldwide?, *Geophys. Res. Lett.*, *23*, 3231–3234.

World Meteorological Organization (WMO) (1999), Scientific assessment of ozone depletion: 1998, Geneva.

Yu, J. R., and C. Y. She (1995), Climatology of a midlatitude mesopause region observed by a lidar at Fort Collins, Colorado (40.6°N, 105°W), *J. Geophys. Res.*, *100*, 7441–7452.

G. P. Brasseur, Max-Planck-Institut für Meteorologie, 20146 Hamburg, Germany. (brasseur@dkrz.de)

A. N. Gruzdev, A. M. Obukhov Institute of Atmospheric Physics, Russian Academy of Sciences, 109017 Moscow, Russia.